Supplemental Material

for

RNA Molecules with Conserved Catalytic Cores but Variable Peripheries Fold along Unique Energetically Optimized Pathways

Somdeb Mitra[1], Alain Laederach[2], Barbara L. Golden[3],

Russ B. Altman[4] and Michael Brenowitz[1,*]

[1]Department of Biochemistry, Albert Einstein College of Medicine, 1300 Morris Park Avenue, Bronx, NY- 10461

[2]Departmnet of Biology, University of North Carolina, CB# 3280, Chapel Hill, NC 27599

[3]Department of Biochemistry, Purdue University, 175 S. University St., West Lafayette, IN-47907-2063

[4]Department of Genetics, Stanford University, 300 Pasteur Drive, Stanford, CA 94305

*Author to whom correspondence should be addressed –

718-430-3179, FAX 718-430-8565, brenowit@aecom.yu.edu

Running head: RNA folding intermediates are optimally stabilized

Key words: Structural homology, RNA folding, kinetic intermediates, group I introns, ribozymes

FIGURE S1A:

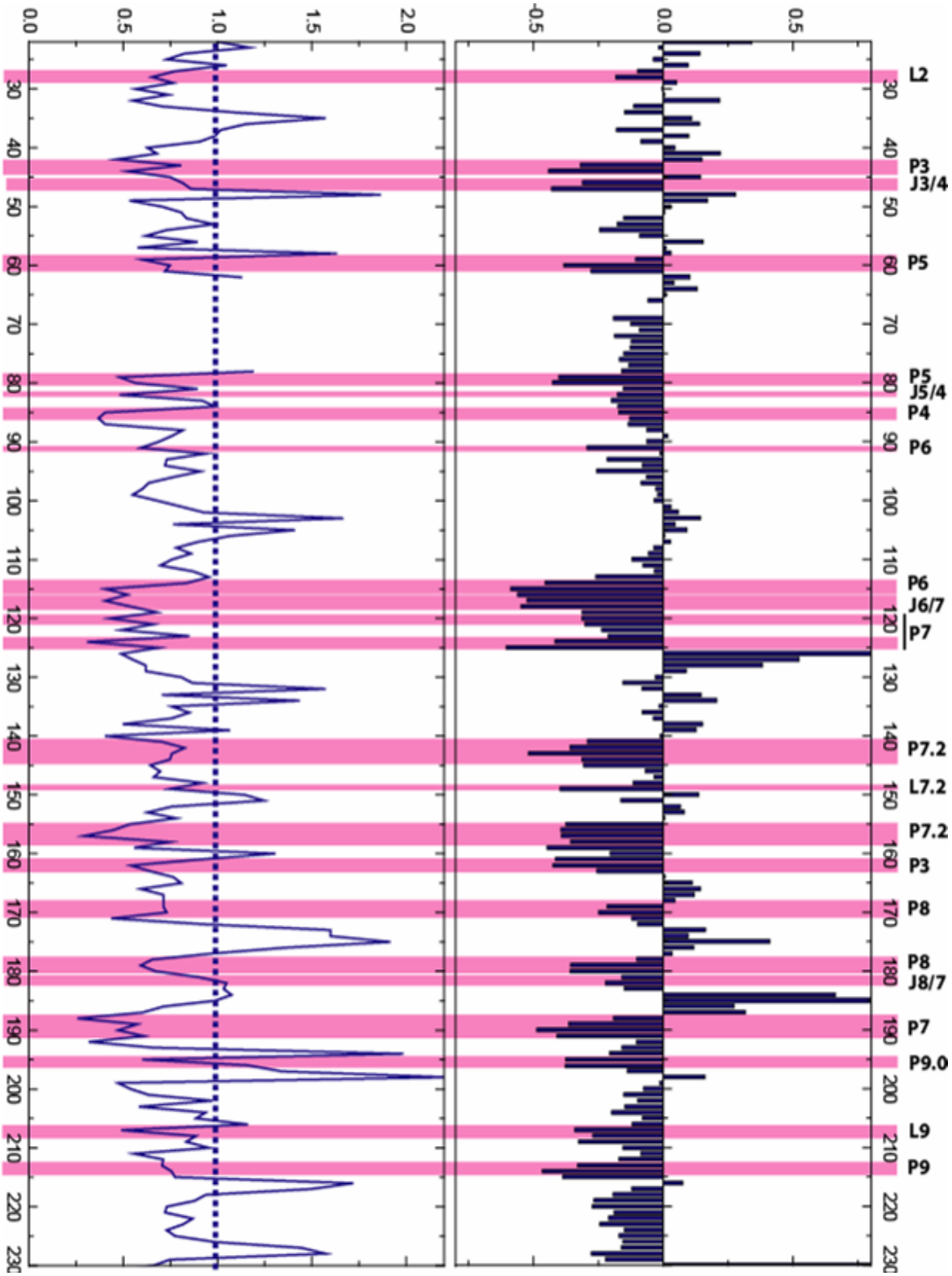
L2
P3
J3/4
P5
P5
J5/4
P4
P6
P6
J6/7
P7
P7.2
L7.2
P7.2
P3
P8
P8
J8/7
P7
P9.0
L9
P9

(A) Correspondence between solvent accessibilities of the backbone of the *Twort* ribozyme measured by $^{\bullet}$OH footprinting (upper panel) and calculated from the crystal structure (lower panel). Each histogram in the upper panel represents the extent of protection of an individual nucleotide in a sample equilibrated at 37^{o}C in 10mM Mg^{2+}, normalized to the extent of protection of the same nucleotide in an unfolded control equilibrated in the absence of Mg^{2+}. Hence, the positive and negative values at each position indicate whether the corresponding nucleotide's backbone is exposed to or buried from the solvent, upon addition of Mg^{2+}, relative to the solvent accessibility of the backbone at the same position in the unfolded RNA. The solid line in the lower panel depicts the solvent accessibilities of the C4' atom in the sugar ring of each nucleotide of the *Twort* ribozyme, calculated from its crystal structure (1Y0Q.pdb) (Golden et al., 2005), relative to the mean solvent accessibility of the C4' atoms of all the nucleotides (shown as the dotted line). The solvent accessibility calculations are performed by rolling sphere of radius 2.8 A^{o} in the software MOLMOL (Koradi et al., 1996). The crests and troughs above and below the dotted line represent residues that are respectively more solvent accessible (less protected) or less solvent accessible (more protected) than an average C4' atom. The pink vertical lines indicate positions that correspond to the formation of native tertiary contacts and were quantitated to yield the time progress curves in the kinetic folding experiments (or folding isotherms in equilibrium folding experiments). The positions of these contacts in the structural context of the ribozyme are indicated above the pink lines in the standard annotation format used to describe the secondary structure of group I intron ribozymes (Michel & Westhof, 1990).

FIGURE S1B:

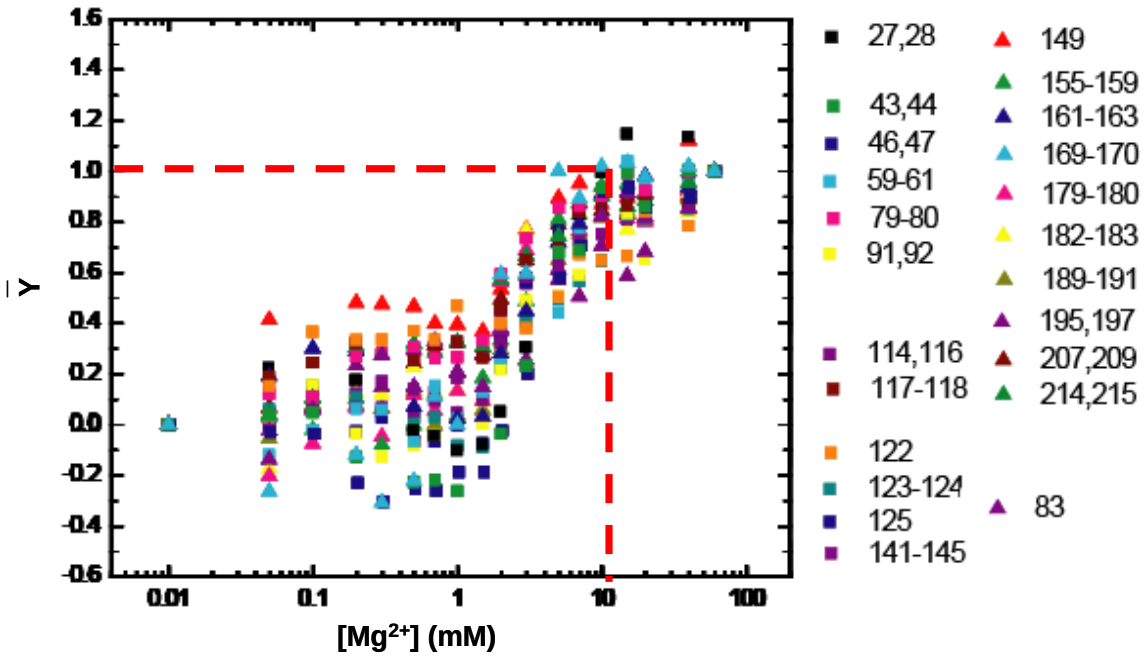

(B) Mg^{2+} mediated equilibrium folding of the Twort ribozyme in CE buffer (10mM Potassium cacodylate, 0.1mM EDTA) containing 100mM KCl. For performing equilibrium $^{\bullet}OH$ footprinting, the ^{32}P-labeled RNA samples were denatured by heating to 95 °C for 2 min in 'CEK Buffer' (10 mM Potassium Cacodylate, 0.1 mM EDTA at pH 7.3, 100 mM KCl) or CE buffer (for monovalent ion titration). The RNA was folded by adding suitable concentrations of $MgCl_2$ (or KCl) and incubated first at 50°C for 30 min followed by 37°C for 1 hour. $^{\bullet}OH$ cleavage was initiated by addition of a solution containing 0.1 mM Fe $(NH_4)_2(SO_4)_2$, 0.14 mM EDTA and 6.6 mM ascorbic acid and allowed to proceed for 30 min. The reaction was quenched by adding 100% ethanol, products were precipitated and separated by 8% denaturing PAGE. The

dried gels were visualized by Storm™ phosphor imaging (GE) and quantitated by the SAFA (Das et al., 2005). Normalized band intensities for the protected residues were plotted as a function of [Mg^{2+}] to obtain titration curves (folding isotherms) which were scaled to fractional saturation by non-linear least squares fitting of the density data against the coupled equations

$$p_i = p_{i,\,lower} + (p_{i,\,upper} - p_{i,\,lower}) \times \overline{Y}_i \qquad \text{eq. 1}$$

and

$$\overline{Y}_i = \frac{K_{di}{}^{n_H}[Mg^{+2}]^{n_H}}{1 + K_{di}{}^{n_H}[Mg^{+2}]^{n_H}} \qquad \text{eq. 2}$$

where *i* denotes a ·OH protection, p_i is the signal quantitated for an *i*, $p_{i,lower}$ and $p_{i,upper}$ are the lower and upper transition endpoints, respectively, K_{di} is the equilibrium disassociation constant, [Mg^{2+}] is the magnesium concentration and n_H is the Hill coefficient. The best-fit values and 65% confidence intervals are reported. Protections from •OH cleavage were identified as described above (in **S1A**), and quantified to generate sets of points depicting the formation of tertiary contacts under equilibrium conditions. Each set of points, representing a tertiary contact, is shown by a different symbol/color on the right side of the graph. The red dotted line indicates that all the tertiary contacts are formed in 10mM Mg^{2+}.

FIGURE S1C:

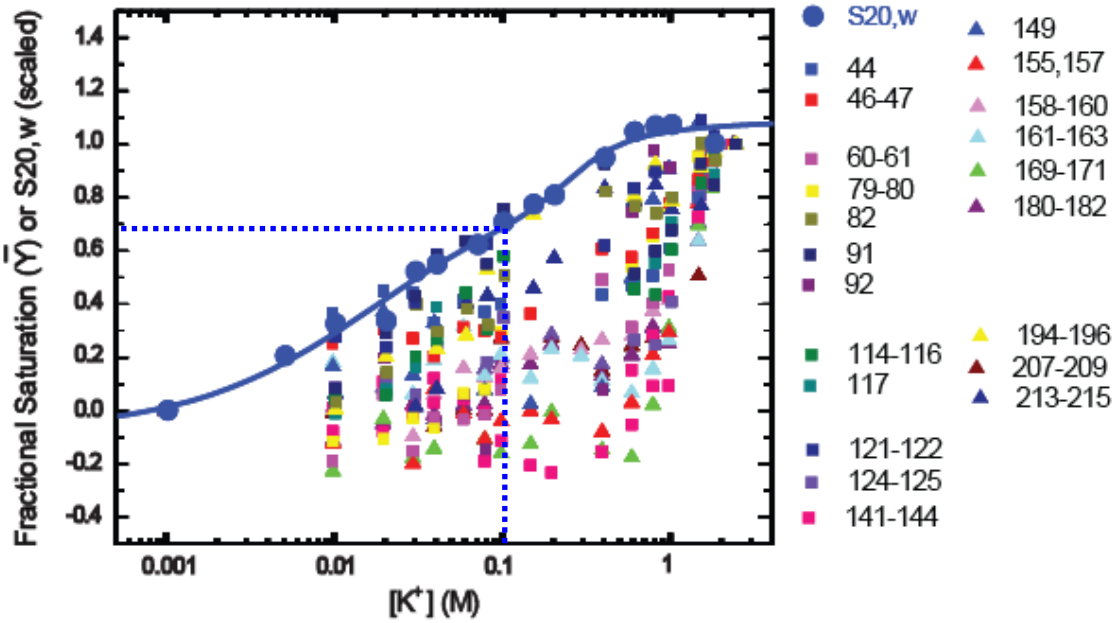

(C) K^+ mediated folding of the Twort ribozyme under equilibrium conditions in 10mM CE buffer. Global compaction (blue filled circles) was measured by analytical ultracentrifugation (AUC) while local tertiary contact formation (filled squares and triangles) was measured by equilibrium ·OH footprinting. Each of the blue filled circles represent the scaled standard sedimentation coefficient (*S*20,w: 20°C in water) of the ribozyme population at a given [K^+]. The AUC experiments were performed at 25°C in CE buffer employing the UV absorption optics (at 260nm) of the Beckman XL-I analytical ultracentrifuge equipped with a An-60 Ti rotor. The absorption scans were analyzed using the software DCDT+ (Philo, 2006) which converts the raw concentration profiles into time derivatives ($\partial c / \partial t$) and fits these values to approximate unbounded solutions of the Lamm equation (Stafford, 1994; Philo, 2000). The fitting yields

values of sedimentation coefficient (*S*) and diffusion coefficient (*D*). The sedimentation coefficients measured at 25^{o}C in CE buffer were converted to their standard values at 20^{o}C in water (*S*20,w) using the program SEDNTERP. An increase in sedimentation coefficient with increasing [K^{+}] indicates that the molecule, starting from an extended structure, progressively assumes a more compact form. The *S*20,w values were scaled between 0 and 1 to overlay the compaction curve on to the footprinting isotherms. The solid blue line is a fit of the AUC data to two consecutive equilibrium transitions with mid points of 0.017±0.001 M and 0.254±0.009 M, respectively. The biphasic monovalent ion mediated equilibrium compaction is reminiscent of a similar behavior observed for the *Tetrahymena* ribozyme(Takamoto et al., 2002). The *Twort* ribozyme achieves full global compaction at lower [K^{+}] than that needed for complete formation of the tertiary contacts. From analogy with the *Tetrahymena* ribozyme, the first phase of *Twort* compaction appears to be due to electrostatic relaxation while the second phase most likely represents further compaction due to tertiary contact formation.

Each set of filled squares and triangles represent the scaled changes in solvent accessibility of a single or a group of nucleotides pertaining to a tertiary contact, as annotated on the right side of the graph. The dotted blue line indicates that the majority of the tertiary contacts are at the most partially formed (between 0% and 40% protection) in 100mM KCl when the first phase of electrostatic relaxation is complete. Only a few backbone regions (nucleotides 91, 114-116, 121-122, 194-196) are protected to a greater extent in 100mM KCl (~60 - 70%). All the remaining tertiary contacts reach their full extent of protection at ~1.5 M [K^{+}]. Therefore the initial state in our experiments (100mM KCl, no Mg^{2+}) represents a predominantly unstructured or very loosely structured, and electrostatically relaxed ensemble of *Twort* ribozyme molecules.

FIGURE S2A:

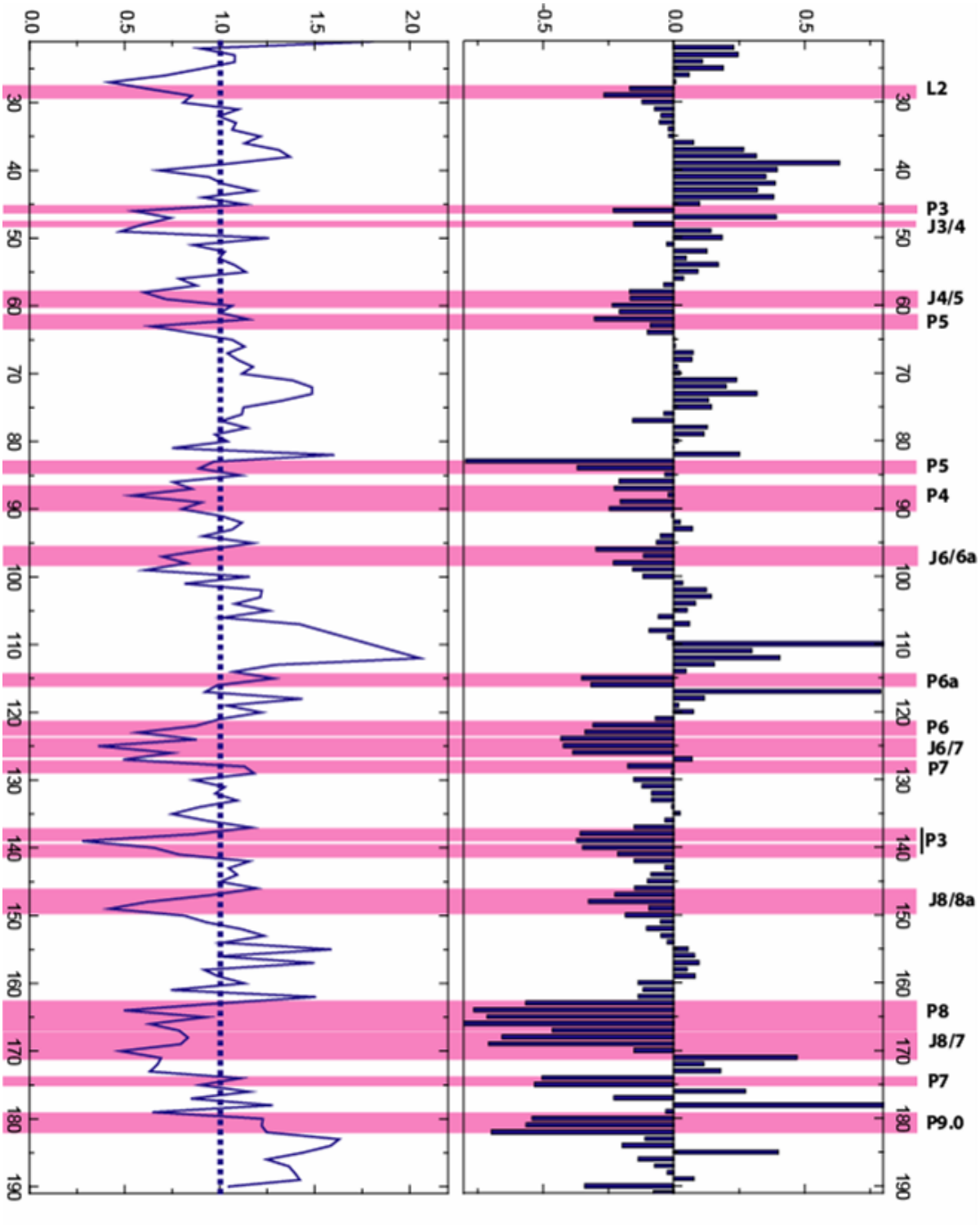

FIGURE S2B:

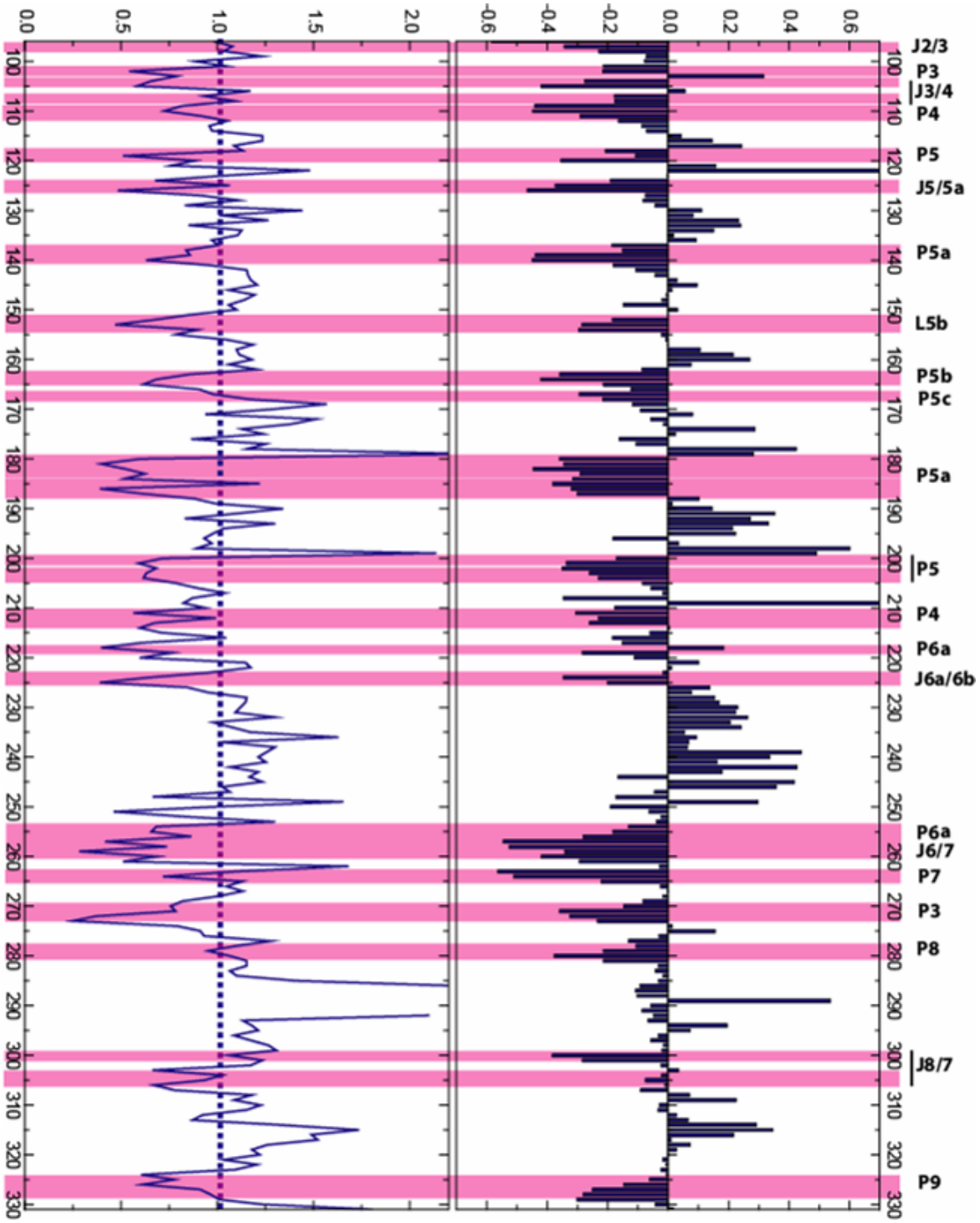
J2/3
P3
J3/4
P4
P5
J5/5a
P5a
L5b
P5b
P5c
P5a
P5
P4
P6a
J6a/6b
P6a
J6/7
P7
P3
P8
J8/7
P9

Correspondence between solvent accessibilities of the backbone of the *Azoarcus* (A) and the *Tetrahymena* (B) ribozymes, measured by •OH footprinting (upper panels) and calculated from the crystal structure (lower panels).The histograms in the upper panels, the solid line in the lower panels, the vertical pink lines, the dotted blue line and the annotations above the top panel represent the same elements as described in Figure S1A. For the *Azoarcus* ribozyme the coordinates from the crystal structure (1ZZN.pdb) (Adams et al., 2004a; Adams et al., 2004b) were used for calculating the C4' atom solvent accessibilities. In case of the *Tetrahymena* ribozyme, for the sake of clarity and accuracy, the C4' atoms of only those residues present in the crystal structure (1X8W.pdb) (Guo et al., 2004) are compared to the corresponding nucleotides' •OH protection patterns in context of the full length ribozyme. We additionally verified that all the protections observed in the full length ribozyme correspond to native tertiary contacts as detected in the well validated 3D model of the full length *Tetrahymena* ribozyme (TtLSU.pdb) (Michel & Westhof, 1990) derived from phylogenetic co-variation analysis.

FIGURE S3:

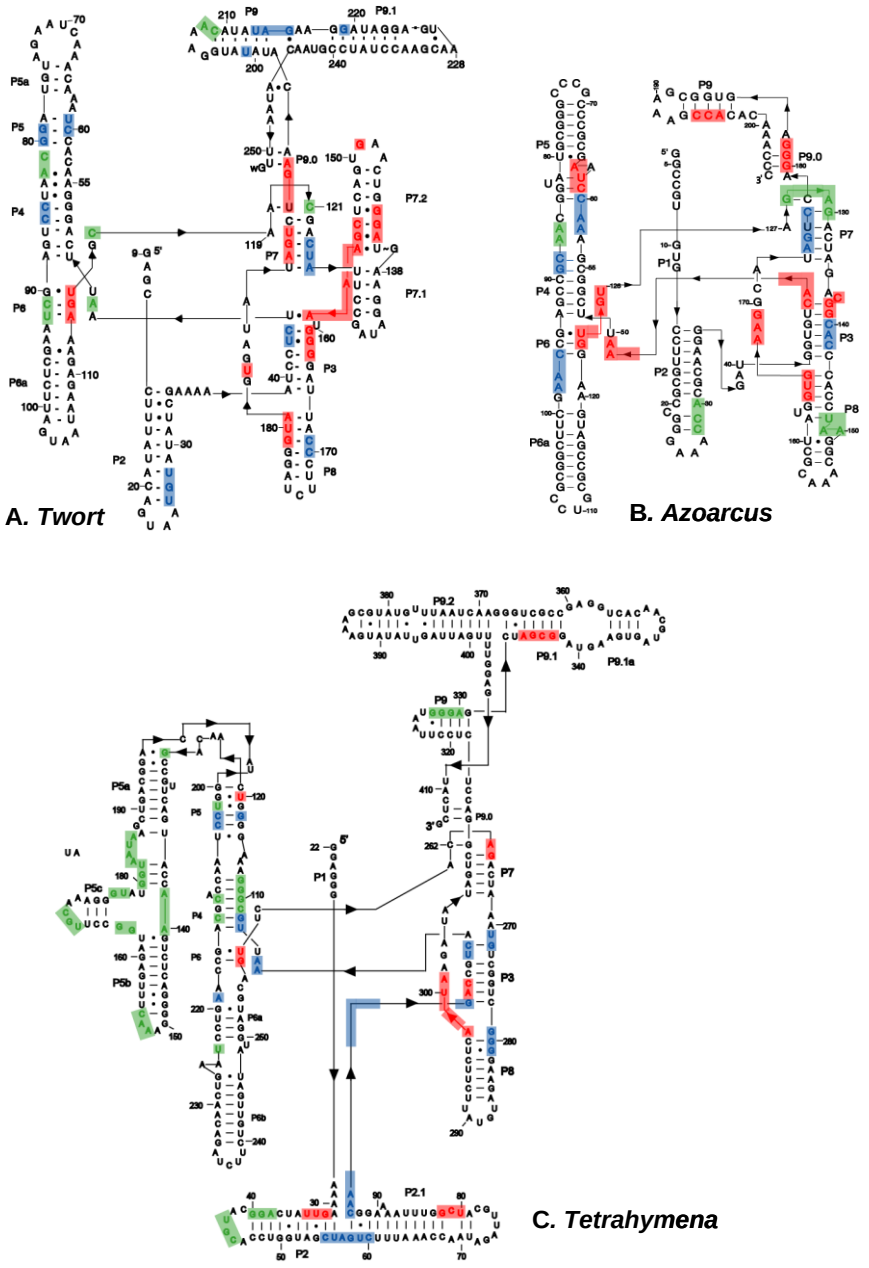

Temporal cluster affiliations of the nucleotides participating in tertiary contacts are mapped on the secondary structures of the **(A)** *Twort*, **(B)** *Azoarcus* and **(C)** *Tetrahymena* ribozymes. Green, red and blue represent the fastest, medium and slowest forming contacts respectively.

FIGURE S4:

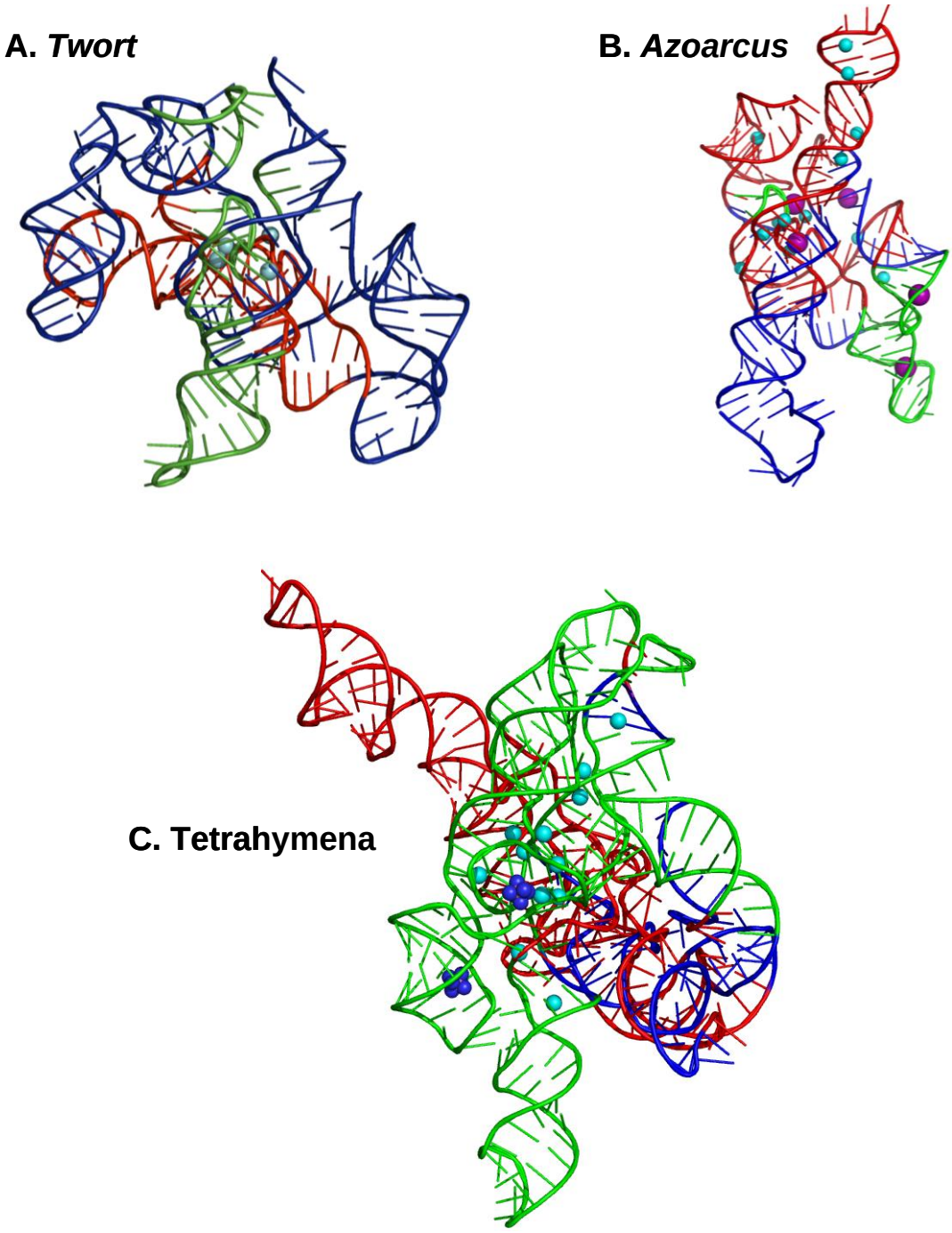

Folded structures (F) derived from Kinfold analysis are represented by mapping all the temporal clusters of tertiary interactions (including the slowest blue clusters not shown in Figure 3 in the main text) on to the crystal structures of the *Twort* **(A)** and *Azoarcus* **(B)** ribozymes and the experimentally validated phylogenetic model of the *Tetrahymena* **(C)** ribozyme. The structures were generated in PYMOL (DeLano, 2009) using co-ordinates obtained from the following PDB entries- **(A)** 1Y0Q (*Twort*) (Golden et al., 2005); **(B)** 1ZZN and 1U6B (*Azoarcus*) (Adams et al., 2004b; Stahley et al., 2007); **(C)** 1X8W (Guo et al., 2004), 1GID (Cate et al., 1996) and TtLSU (Michel & Westhof, 1990) (*Tetrahymena*). The positions of divalent and monovalent ions (when known in the crystal structures) are indicated by cyan and purple spheres respectively. The groups of dark blue spheres in the *Tetrahymena* ribozyme represent cobalt hexammine molecules observed in the crystal structure of its P4-P6 domain (1GID.pdb) (Cate et al., 1997) and denote sites that bind hydrated magnesium ions. To represent the folded state of the full length *Tetrahymena* ribozyme with bound ions, as accurately as possible, the three structures 1X8W (partial structure of the *Tetrahymena* ribozyme), 1GID (P4-P6 domain of the *Tetrahymena* ribozyme) and TtLSU (phylogenetically derived full length 3D model of the *Tetrahymena* ribozyme) were aligned using conserved residues that are common to all the three structures.

FIGURE S5:

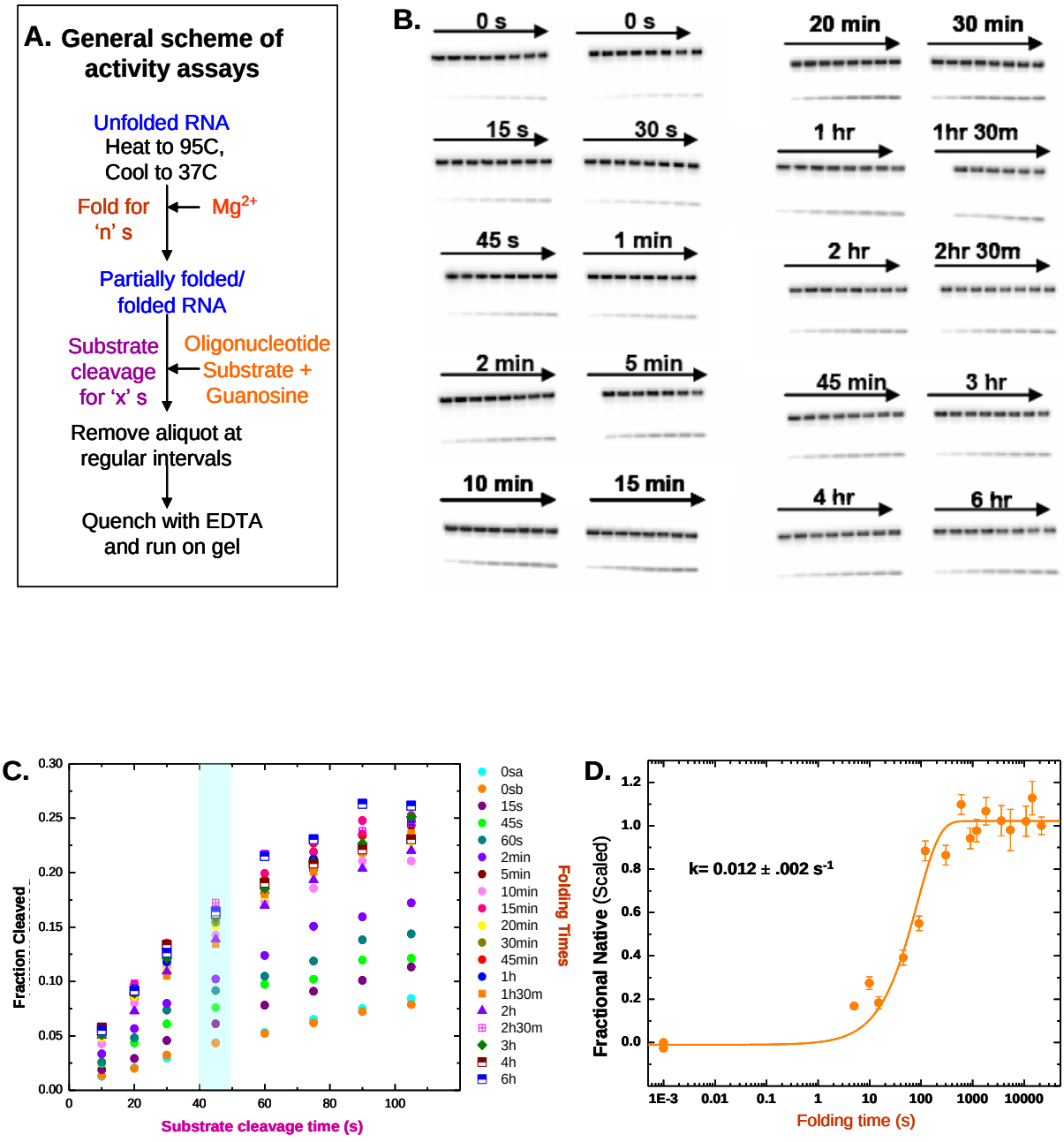
A. General scheme of activity assays
Unfolded RNA
Heat to 95C,
Cool to 37C
Fold for 'n' s
Mg2+
Partially folded/ folded RNA
Substrate cleavage for 'x' s
Oligonucleotide Substrate + Guanosine
Remove aliquot at regular intervals
Quench with EDTA and run on gel
B.
0 s
0 s
20 min
30 min
15 s
30 s
1 hr
1hr 30m
45 s
1 min
2 hr
2hr 30m
2 min
5 min
45 min
3 hr
10 min
15 min
4 hr
6 hr
C.
Fraction Cleaved
Substrate cleavage time (s)
0sa
0sb
15s
45s
60s
2min
5min
10min
15min
20min
30min
45min
1h
1h30m
2h
2h30m
3h
4h
6h
Folding Times
D.
Fractional Native (Scaled)
k= 0.012 ± .002 s-1
Folding time (s)

(A) General scheme of the catalytic activity assays. **(B-D) Summary of the *Azoarcus* ribozyme activity assays. (A)** The general reaction scheme for determining the time dependent evolution of the catalytically active native state of a ribozyme is depicted. We essentially perform these experiments as designed by Yuan and Russell (personal communication) for the *Azoarcus* ribozyme and as described by (Zarrinkar & Williamson, 1994a) for the *Tetrahymena* and the *Twort* ribozymes. The unfolded RNA (in CE buffer + 100mM KCl) is heat denatured at 95^{o}C for 3 minutes and cooled to 37 ^{o}C. The RNA sample is mixed with 10mM $MgCl_2$ solution (hand mixing for slower time points and quench flow mixing for faster time points) and allowed to age for a given time period (folding time of 'n' seconds). At the end of each folding time period a certain fraction of molecules reaches the catalytically active native state which is monitored by adding an oligo-nucleotide substrate (containing mostly unlabeled substrate with a trace amount of substrate radioactively labeled at the 5' end) along with an exogenous nucleophile (guanosine). The population of ribozyme molecules that correctly fold to the native state (during the n^{th} folding period) binds and rapidly cleaves a fraction of the supplied oligo-nucleotide substrate (Herschlag & Cech, 1990; Russell & Herschlag, 1999b). This substrate cleavage reaction (for each of the folding time periods) is usually allowed to proceed for 2 minutes during which aliquots are removed at intervals of 10-15 seconds, quenched with twice the volume of a solution containing EDTA, formamide loading buffer and gel loading dyes. The quenched reaction time points are run through a denaturing polyacrylamide gel to separate the cleaved product from the intact substrate and thereby quantitate the fraction of substrate cleaved at a given reaction time point. The fraction of native ribozyme present at the end of a folding time point 'n' is estimated from the amplitude of the product burst from the substrate cleavage reaction for the n^{th} folding time point. For estimating the product burst, we usually consider the

30 second cleavage reaction time point, following (Zarrinkar & Williamson, 1994a; Treiber et al., 1998b). In order to balance signal strength and speed of the cleavage reaction, the reactions are performed not under strictly multiple turn-over conditions but with a 2 to 5 fold stoichiometric excess of the substrate over the ribozyme. The '0' second time point, representing the initial state of the folding reaction, is obtained by initiating the cleavage reaction simultaneously with the initiation of the folding reaction by addition of Mg^{2+}. The end point of the folding reaction is obtained by pre-equilibrating a ribozyme sample for 30 minutes 50^{o}C and 2 hours at 37^{o}C in 10mM $MgCl_2$. **(B)** Sample gels from the activity assays of the *Azoarcus* ribozyme are shown. In each lane, the upper bands (larger oligo) represent the uncut labeled substrate while the lower bands (smaller oligo) represent the cleaved product. Each set of 8 lanes represent the cleavage reactions for a given folding time point 'n', indicated by the numbers above the arrows (the arrows indicate progress of the cleavage reaction from left to right). **(C)** The fraction of substrate cleaved as a function of cleavage time points, for each folding reaction, is plotted. Each folding reaction is represented by a symbol of a different shape/color, as shown on the right side of the graph. **(D)** Time dependent evolution of the native *Azoarcus* ribozyme is obtained by plotting the fraction of substrate cleaved at the same cleavage time point (30 seconds in this case) for all the folding time points. The error bars are derived from three independent measurements. The data are fit to a single exponential to obtain the first order rate constant, k= 0.012 s^{-1}, of overall folding of the *Azoarcus* ribozyme to the native state.

FIGURE S6:

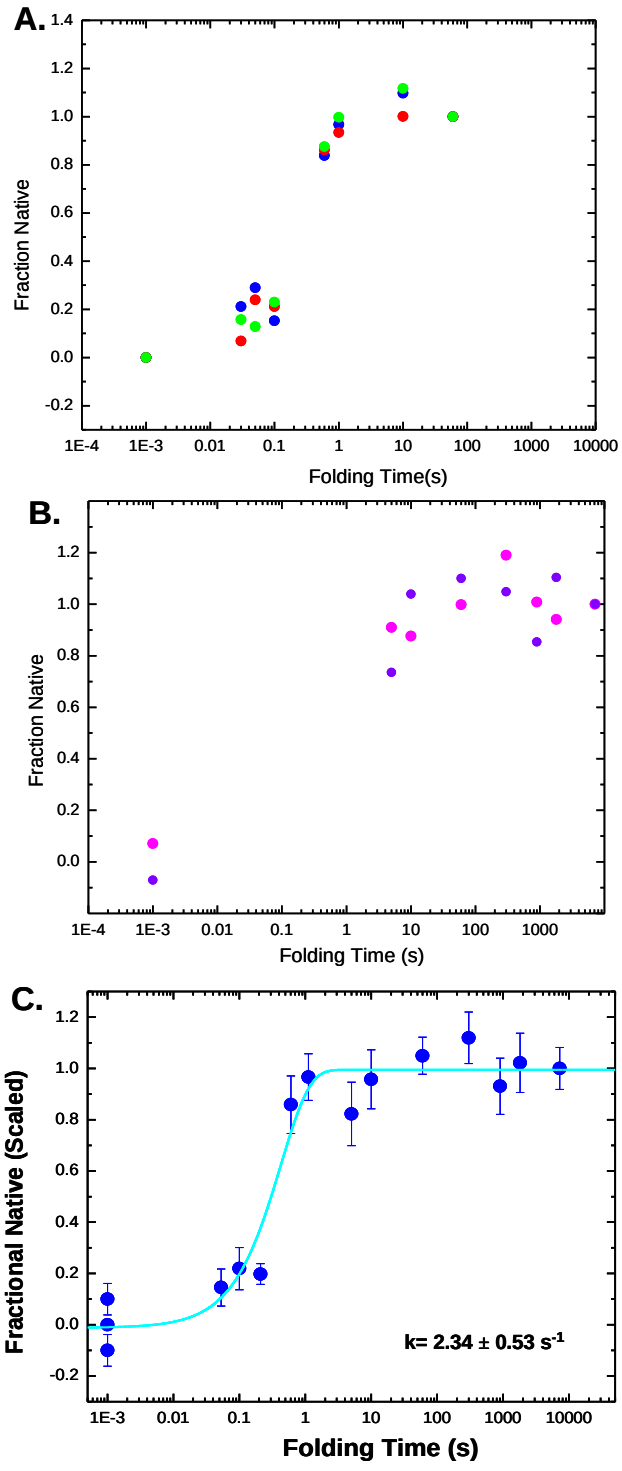
A.
Fraction Native
Folding Time(s)
B.
Fraction Native
Folding Time (s)
C.
Fractional Native (Scaled)
k= 2.34 ± 0.53 s-1
Folding Time (s)

Catalytic activity assays for the *Twort* ribozyme. **(A)** To monitor the time dependent evolution of the native state in the millisecond time regime, we resorted to rapid quench flow mixing of the ribozyme and the folding buffer (containing $MgCl_2$) prior to initiation of the cleavage reaction reagents; as described in (Shcherbakova et al., 2004). Briefly, the ribozyme (dissolved in CE buffer with 100mM KCl) and the folding buffer (containing $MgCl_2$) are driven from the two sample syringes in to the mixing chamber of the Kintek® quench flow apparatus and allowed to age for a defined time interval (folding time 'n'). At the end of the folding time period the entire reaction is mix is rapidly ejected in to a tube containing the oligo substrate and the guanosine nucleophile, to initiate the cleavage reaction. Reaction aliquots are removed at regular intervals, quenched and analysis of the cleavage products is performed as described above. The results of three independent measurements are shown in the plot. **(B)** To determine the slower steps of appearance of the native ribozyme we used the previously described standard hand-mixing assay. Results of two independent measurements are shown. **(C)** The data from the two experiments were combined by averaging the overlapping time points from the two assays. The data were fit to a single exponential to obtain the first order rate constant, k= 2.34 s^{-1}, of overall folding of the *Twort* ribozyme to the native state.

FIGURE S7:

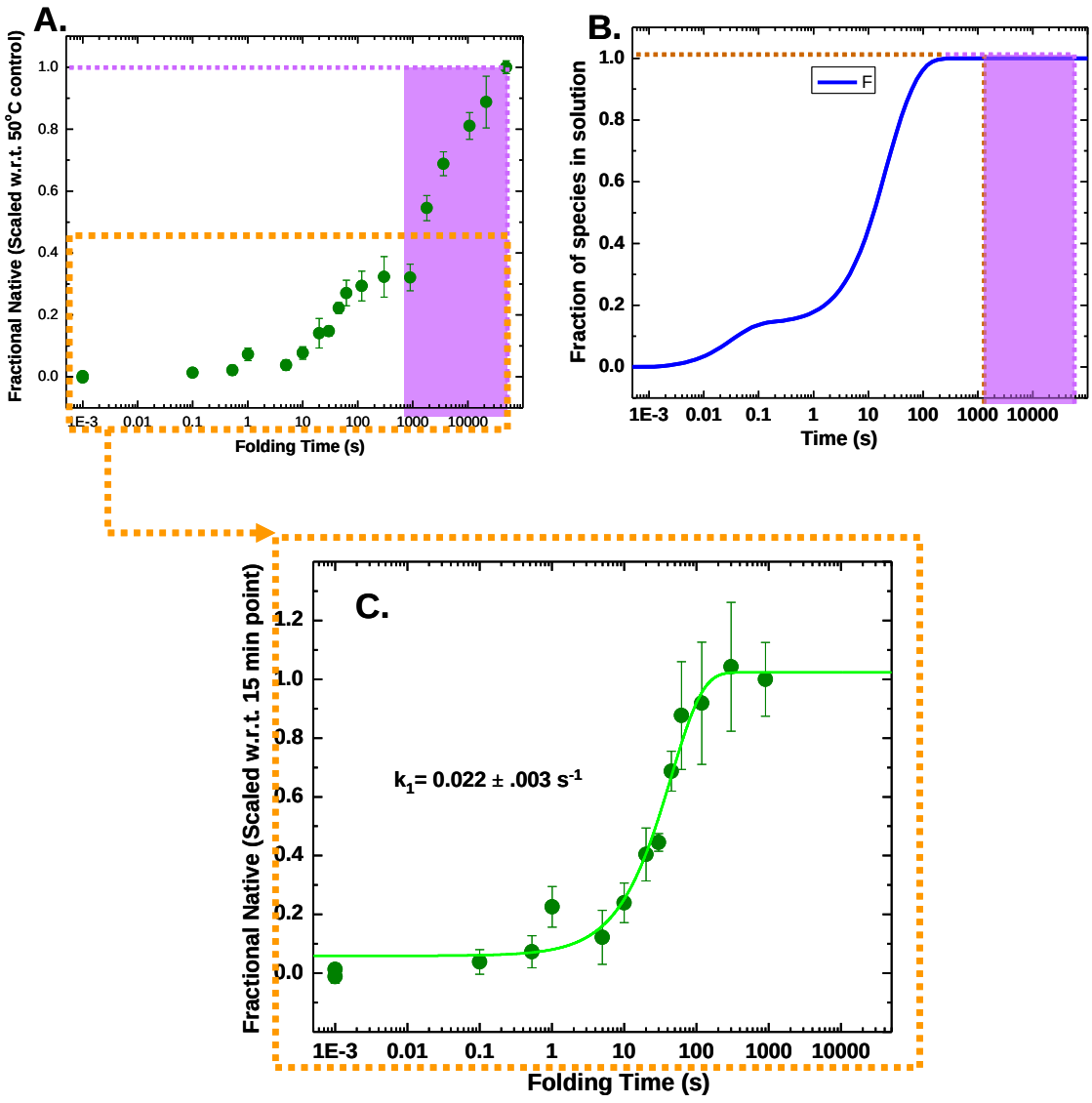

Catalytic activity assays for the *Tetrahymena* ribozyme were performed as described in (Zarrinkar & Williamson, 1994a; Treiber et al., 1998a). The presence of a highly paradoxical long lived misfolded intermediate 'M' has been well documented for the *Tetrahymena* ribozyme (Russell et al., 2006) and it has been independently verified by several groups that under standard folding conditions (37°C or 42°C, 10 mM Mg^{2+}, pH 7.3 and 50 to 100mM monovalent ions), the ribozyme acquires between 25 to 50% of its full activity (Russell & Herschlag, 1999a;

Russell & Herschlag, 2001; Treiber & Williamson, 2001; Russell et al., 2002; Uchida et al., 2003). The 'M' state is virtually indistinguishable from the native ribozyme by chemical structure probing methods like $^{\bullet}$OH footprinting (Russell et al., 2006). **(A)** Our activity assay over an extended time period shows that fully active native state appears in two phases, a fast initial phase during which about 30% of the ribozyme reaches the catalytically active native state and a second slow phase during which the remaining 70% of the ribozyme reaches the catalytically active native state. The second phase presumably involves conversion of the 'M' state to the native state. The data has been scaled with respect to the fully folded control at 50^{o}C (last point indicated by the purple dotted line). The error bars are calculated from three independent measurements. The area shaded in purple corresponds to the time regime during which approximately 70% of the ribozyme slowly reaches full catalytic activity. **(B)** Time dependent evolution of the fully folded species 'F', as calculated from the structural-kinetic models of the *Tetrahymena* ribozyme. The brown dotted lines indicate that formation of native tertiary structure is complete within ~3.3 min. The area shaded in purple corresponds to the second slow phase observed in activity assays during which no changes are detectable in back-bone solvent accessibilities (as measured by $^{\bullet}$OH footprinting). **(C)** The initial phase of time dependent evolution of approximately 30% of the active ribozyme, scaled with respect to the end point of this phase (15 min). This phase when fit as a single exponential, yields a rate constant k= 0.025 s^{-1} which is very similar to the values obtained in previous studies(Zarrinkar & Williamson, 1994a; Zarrinkar & Williamson, 1994b; Rook et al., 1999; Treiber & Williamson, 2001; Laederach et al., 2006; Russell et al., 2006). This first phase shows a good agreement with the rate of native tertiary structure formation derived from Kinfold analysis, as shown in Figure 4C of the main text.

TABLE S1:

Twort		Azoarcus		Tetrahymena	
Cluster & Defined Region	Backbone Positions Protected from •OH cleavage	Cluster & Defined Region	Backbone Positions Protected from •OH cleavage	Cluster & Defined Region	Backbone Positions Protected from •OH cleavage
70 Green	47 81,82 91,92 118,121 208,209	Green	28,29,30 86,87 128,129,130 148,149,150, 151,152	Green	38, 39,40 43,44,45 109,110,111,112 126 139,140 152,153,154 163,164 168,169,170 176,177 180,181,182 183,184,185,186 202 211, 213 224 327,328,329,330
Red	114,115,116 141,142,143 155,156,157,158,159 161,162,163 179,180,181,183 189,190,191 193,194,195	Red	46,47 48,49 61,62,64 123,124,125, 126 137,138,139 167,168,169 180,181,182 194,195,196	Red	32,33,34 59,60 80,81,82 97,98 120 257,258 263,264 299,300,301 343,344,345,346
Blue	26,28 43,44 60,61 79,80 85,86 124,125,126 169,170 201 213,214,215 219	Blue	 58,59,60 88,89 96,97,98 140,141,142 174,175,177	Blue	 55,56,57,58 93,94,95,96 101,102 104,105 107,108 118 203,204 219 271,272 279,280,281

TABLE S2:

A. *Twort*

	U	**I1**	**I2**	**F**
U		100±5	59±4	18±2
I1	0.01±0.01		0.0±0.2	1.5±0.5
I2	0.01±0.01	0.0±0.2		2.5±0.5
F	0.01±0.01	0.05±0.05	0.01±0.01	

B. *Azoarcus*

	U	**I1**	**I2**	**F**
U		43±6	39±1	3.2±0.01
I1	0.01±0.01		0.002±0.001	0.03±0.003
I2	0.01±0.01	0.001±0.001		0.003±0.0003
F	0.001±0.001	0.01±0.01	0.01±0.01	

C. *Tetrahymena*

	U	**I1**	**I2**	**F**
U		12±1	15±1.5	4±0.3
I1	0.001±0.001		0.1±0.02	0.02±0.01
I2	0.0001±0.0001	0.06±0.02		0.07±0.02
F	0.001±0.001	0.001±0.001	0.001±0.001	

We report here the rates for the three kinetic models for *Twort*, *Azoarcus*, and *Tetrahymena* without applying bounds to the reverse rates. In all cases the reverse rates are close to zero and poorly determined. These rates are difficult to determine due to the progression of all our reactions to full completion (saturation of protection), which results in small values for the reverse rates. We choose to bind these values to zero in the models we report, as this reduces the dimensionality of the optimization problem resulting in overall lower error on the forward rates.

Reference

Adams P, Stahley M, Gill M, Kosek A, Wang J, Strobel S. 2004a. Crystal structure of a group I intron splicing intermediate. *RNA 10*:1867-1887.

Adams P, Stahley M, Kosek A, Wang J, Strobel S. 2004b. Crystal structure of a self-splicing group I intron with both exons. *Nature 430*:45-50.

Cate J, Gooding A, Podell E, Zhou K, Golden B, Kundrot C, Cech T, Doudna J. 1996. Crystal structure of a group I ribozyme domain: principles of RNA packing. *Science 273*:1678-1685.

Cate J, Hanna R, Doudna J. 1997. A magnesium ion core at the heart of a ribozyme domain. *Nat Struct Biol 4*:553-558.

Das R, Laederach A, Pearlman SM, Herschlag D, Altman RB. 2005. SAFA: semi-automated footprinting analysis software for high-throughput quantification of nucleic acid footprinting experiments. *RNA 11*:344-354.

DeLano WL. 2009. The PyMOL Molecular Graphics System, http://www.pymol.org. Palo Alto, California: DeLano Scientific LLC.

Golden BL, Kim H, Chase E. 2005. Crystal structure of a phage Twort group I ribozyme-product complex. *Nat Struct Mol Biol 12*:82-89.

Guo F, Gooding AR, Cech TR. 2004. Structure of the Tetrahymena ribozyme: base triple sandwich and metal ion at the active site. *Mol Cell 16*:351-362.

Herschlag D, Cech TR. 1990. Catalysis of RNA cleavage by the Tetrahymena thermophila ribozyme. 1. Kinetic description of the reaction of an RNA substrate complementary to the active site. *Biochemistry 29*:10159-10171.

Koradi R, Billeter M, Wuthrich K. 1996. MOLMOL: a program for display and analysis of macromolecular structures. *J Mol Graph 14*:51-55, 29-32.

Laederach A, Shcherbakova I, Liang M, Brenowitz M, Altman R. 2006. Local kinetic measures of macromolecular structure reveal partitioning among multiple parallel pathways from the earliest steps in the folding of a large RNA molecule. *J Mol Biol 358*:1179-1190.

Michel F, Westhof E. 1990. Modelling of the three-dimensional architecture of group I catalytic introns based on comparative sequence analysis. *J Mol Biol 216*:585-610.

Philo JS. 2000. A method for directly fitting the time derivative of sedimentation velocity data and an alternative algorithm for calculating sedimentation coefficient distribution functions. *Anal Biochem 279*:151-163.

Philo JS. 2006. Improved methods for fitting sedimentation coefficient distributions derived by time-derivative techniques. *Anal Biochem 354*:238-246.

Rook MS, Treiber DK, Williamson JR. 1999. An optimal Mg(2+) concentration for kinetic folding of the tetrahymena ribozyme. *Proc Natl Acad Sci U S A 96*:12471-12476.

Russell R, Das R, Suh H, Travers KJ, Laederach A, Engelhardt MA, Herschlag D. 2006. The paradoxical behavior of a highly structured misfolded intermediate in RNA folding. *J Mol Biol 363*:531-544.

Russell R, Herschlag D. 1999a. New pathways in folding of the Tetrahymena group I RNA enzyme. *J Mol Biol 291*:1155-1167.

Russell R, Herschlag D. 1999b. New pathways in folding of the Tetrahymena group I RNA enzyme. *J Mol Biol 291*:1155-1167.

Russell R, Herschlag D. 2001. Probing the folding landscape of the Tetrahymena ribozyme: commitment to form the native conformation is late in the folding pathway. *J Mol Biol 308*:839-851.

Russell R, Zhuang X, Babcock HP, Millett IS, Doniach S, Chu S, Herschlag D. 2002. Exploring the folding landscape of a structured RNA. *Proc Natl Acad Sci U S A 99*:155-160.

Shcherbakova I, Gupta S, Chance M, Brenowitz M. 2004. Monovalent ion-mediated folding of the Tetrahymena thermophila ribozyme. *J Mol Biol 342*:1431-1442.

Stafford WF, 3rd. 1994. Boundary analysis in sedimentation velocity experiments. *Methods Enzymol 240*:478-501.

Stahley MR, Adams PL, Wang J, Strobel SA. 2007. Structural metals in the group I intron: a ribozyme with a multiple metal ion core. *J Mol Biol 372*:89-102.

Takamoto K, He Q, Morris S, Chance MR, Brenowitz M. 2002. Monovalent cations mediate formation of native tertiary structure of the Tetrahymena thermophila ribozyme. *Nat Struct Biol 9*:928-933.

Treiber D, Rook M, Zarrinkar P, Williamson J. 1998a. Kinetic intermediates trapped by native interactions in RNA folding. *Science 279*:1943-1946.

Treiber DK, Rook MS, Zarrinkar PP, Williamson JR. 1998b. Kinetic intermediates trapped by native interactions in RNA folding. *Science 279*:1943-1946.

Treiber DK, Williamson JR. 2001. Concerted kinetic folding of a multidomain ribozyme with a disrupted loop-receptor interaction. *J Mol Biol 305*:11-21.

Uchida T, Takamoto K, He Q, Chance M, Brenowitz M. 2003. Multiple monovalent ion-dependent pathways for the folding of the L-21 Tetrahymena thermophila ribozyme. *J Mol Biol 328*:463-478.

Zarrinkar P, Williamson J. 1994a. Kinetic intermediates in RNA folding. *Science 265*:918-924.

Zarrinkar PP, Williamson JR. 1994b. Kinetic intermediates in RNA folding. *Science 265*:918-924.